

# Chaotic Mixing in a Torus Map

Jean-Luc Thiffeault\*

*Department of Applied Physics and Applied Mathematics,  
Columbia University, New York, NY 10027<sup>†</sup>*

Stephen Childress<sup>‡</sup>

*Courant Institute of Mathematical Sciences,  
New York University, New York, NY 10012*

(Dated: November 2, 2018)

The advection and diffusion of a passive scalar is investigated for a map of the 2-torus. The map is chaotic, and the limit of almost-uniform stretching is considered. This allows an analytic understanding of the transition from a phase of constant scalar variance (for short times) to exponential decay (for long times). This transition is embodied in a short superexponential phase of decay. The asymptotic state in the exponential phase is an eigenfunction of the advection–diffusion operator, in which most of the scalar variance is concentrated at small scales, even though a large-scale mode sets the decay rate. The duration of the superexponential phase is proportional to the logarithm of the exponential decay rate; if the decay is slow enough then there is no superexponential phase at all.

PACS numbers: 47.52.+j, 05.45.-a

Keywords: chaotic mixing, advection–diffusion, torus maps

**A crucial problem involving fluids in the physical sciences is to understand the nature of mixing—its efficiency and thoroughness. Examples range from the mundane (cream in coffee), to the utilitarian (temperature in room), the industrial (mixing in chemical reactors), and the planetary (mixing of ozone in the extratropical stratosphere). If the flow is not turbulent, mixing can nevertheless be very efficient, due to a phenomenon called chaotic advection. In that case, the flow appears regular, but individual fluid trajectories are very complicated and lead to a stretching and folding action that greatly enhances mixing. Here we discuss mixing for a simple map, and show that a large-scale, coherent pattern is created that dominates the diffusive process.**

## I. INTRODUCTION

It has recently been suggested<sup>1,2</sup> that estimates of the decay rate of the variance of a passive scalar under the effect of advection and diffusion<sup>3–6</sup> do not yield satisfactory results when applied to some simple maps, such as the inhomogeneous baker’s map.<sup>7–9</sup> This also

---

\*Electronic address: [jeanluc@mailaps.org](mailto:jeanluc@mailaps.org)

<sup>†</sup>Present address: Department of Mathematics, Imperial College London, SW7 2AZ, United Kingdom

<sup>‡</sup>Electronic address: [childress@cims.nyu.edu](mailto:childress@cims.nyu.edu)

seems to be the case in laboratory experiments on periodic flows,<sup>10,11</sup> where the decay rate is observed to be about an order of magnitude slower than the decay rate based on local arguments, such as the distribution of Lyapunov exponents.<sup>12</sup> Part of the reason for this is that in chaotic advection<sup>13</sup> (*i.e.*, smooth flows with chaotic Lagrangian trajectories), far from the highly-turbulent regime, the presence of slowly-decaying eigenfunctions dominates the long-time decay rate.<sup>1,2,14–16</sup> (For the experiments, the presence of regular islands and barriers is also crucial, but we shall not address this complicated and poorly-understood issue here. It suffices to observe that the concentration field clearly attains an eigenfunction-like regime.<sup>14</sup>) The existence of such eigenfunctions of the advection–diffusion operator was demonstrated convincingly via a numerical approach for the inhomogeneous baker’s map.<sup>1,2</sup> Sukhatme and Pierrehumbert<sup>17</sup> explained that the discrepancy is not due to a failure of the local approaches, but because they assume that the initial scale of variation of the passive scalar is much smaller than the system size.

Here we propose to use a diffeomorphism of the 2-torus (an extension of Arnold’s cat map<sup>18</sup>) to further investigate aspects of the decay of variance and provide some analytical results. We find that, when the map is close to uniformly stretching, the decay rate is much faster than indicated by the distribution of Lyapunov exponents, as was also found in the inhomogeneous baker’s map.<sup>1</sup> In Fereday et al.<sup>1</sup> and laboratory experiments,<sup>12</sup> a slower decay was also observed, but far from the uniformly-stretching (homogeneous) regime.

The paper is organized as follows. In Section II we introduce the map and derive basic expressions for the effect of advection and diffusion on a passive scalar. We then analyze the superexponential (Section III) and exponential (Section IV) phases of diffusion. The spectrum of variance for the exponential eigenfunction is derived in Section V, followed by a discussion of the results in Section VI.

## II. ADVECTION–DIFFUSION IN A MAP

We consider a diffeomorphism of the 2-torus  $\mathcal{T}^2 = [0, 1]^2$ ,

$$\mathcal{M}(\mathbf{x}) = \mathbb{M} \cdot \mathbf{x} + \boldsymbol{\phi}(\mathbf{x}), \quad (1)$$

where  $\mathbb{M}$  is a  $2 \times 2$  nonsingular matrix with integer coefficients and  $\boldsymbol{\phi}(\mathbf{x})$  is periodic in both directions with unit period. We choose  $\mathbb{M}$  to have unit determinant, with an eigenvalue larger than one and the other less than one, so that even in absence of the  $\boldsymbol{\phi}$  term  $\mathcal{M}$  is still chaotic. Specifically, we take

$$\mathbb{M} = \begin{pmatrix} 2 & 1 \\ 1 & 1 \end{pmatrix}; \quad \boldsymbol{\phi}(\mathbf{x}) = \frac{K}{2\pi} \begin{pmatrix} \sin 2\pi x_1 \\ \sin 2\pi x_1 \end{pmatrix}; \quad (2)$$

so that  $\mathbb{M} \cdot \mathbf{x}$  is the Arnold cat map and  $\boldsymbol{\phi}$  is a wave term usually associated with the standard map. The map  $\mathcal{M}$  is area-preserving, and for  $K = 0$  the stretching of phase-space elements is uniform in space. The map is always chaotic (the largest Lyapunov exponent is positive). For small  $K$ , there are no barriers to transport, such as islands, often encountered in realistic flows.

We consider the effect of iterating the map and applying the heat operator to a scalar distribution  $\theta^{(i-1)}(\mathbf{x})$ ,

$$\theta^{(i)}(\mathbf{x}) = \mathcal{H}_e \theta^{(i-1)}(\mathcal{M}^{-1}(\mathbf{x})), \quad (3)$$

where  $\epsilon$  is the diffusivity, and the heat operator  $\mathcal{H}_\epsilon$  and kernel  $h_\epsilon$  are

$$\mathcal{H}_\epsilon \theta(\mathbf{x}) := \int_{\mathcal{T}^2} h_\epsilon(\mathbf{x} - \mathbf{y}) \theta(\mathbf{y}) d\mathbf{y}; \quad h_\epsilon(\mathbf{x}) = \sum_{\mathbf{k}} \exp(2\pi i \mathbf{k} \cdot \mathbf{x} - \mathbf{k}^2 \epsilon). \quad (4)$$

We Fourier expand  $\theta^{(i)}(\mathbf{x})$ ,

$$\theta^{(i)}(\mathbf{x}) = \sum_{\mathbf{k}} \hat{\theta}_{\mathbf{k}}^{(i)} e^{2\pi i \mathbf{k} \cdot \mathbf{x}} \quad (5)$$

so that (3) becomes

$$\hat{\theta}^{(i)}(\mathbf{x}) = \sum_{\mathbf{q}} \mathbb{T}_{\mathbf{kq}} \hat{\theta}_{\mathbf{q}}^{(i-1)}, \quad (6)$$

with the transfer matrix,

$$\mathbb{T}_{\mathbf{kq}} := \int_{\mathcal{T}^2} \exp(2\pi i (\mathbf{q} \cdot \mathbf{x} - \mathbf{k} \cdot \mathcal{M}(\mathbf{x})) - \epsilon \mathbf{q}^2) d\mathbf{x}. \quad (7)$$

We may regard  $\mathbf{q}$  as the ‘‘initial’’ wavenumber, and  $\mathbf{k}$  as the ‘‘final’’ one, with a nonzero  $\mathbb{T}_{\mathbf{kq}}$  denoting a transfer of concentration from  $\mathbf{q}$  to  $\mathbf{k}$  under one application of the map.

For the form of the map given by (1) and (2), we have

$$\mathbb{T}_{\mathbf{kq}} = e^{-\epsilon \mathbf{q}^2} \int_{\mathcal{T}^2} \exp(2\pi i (\mathbf{q} - \mathbf{k} \cdot \mathbb{M}) \cdot \mathbf{x} - i(k_1 + k_2)K \sin(x_1)) d\mathbf{x}. \quad (8)$$

The integral in  $x_2$  gives a Kronecker delta, and the  $x_1$  integral is readily written as a Bessel function; we thus have

$$\mathbb{T}_{\mathbf{kq}} = e^{-\epsilon \mathbf{q}^2} \delta_{0, Q_2} i^{Q_1} J_{Q_1}((k_1 + k_2)K), \quad \mathbf{Q} := \mathbf{k} \cdot \mathbb{M} - \mathbf{q}, \quad (9)$$

where the  $J_Q$  is a Bessel function of the first kind.

In the absence of diffusion ( $\epsilon = 0$ ), the variance

$$\sigma^{(i)} := \int_{\mathcal{T}^2} |\theta^{(i)}(\mathbf{x})|^2 d\mathbf{x} = \sum_{\mathbf{k}} \sigma_{\mathbf{k}}^{(i)}; \quad \sigma_{\mathbf{k}}^{(i)} := |\hat{\theta}_{\mathbf{k}}^{(i)}|^2, \quad (10)$$

is preserved by (3) (we assume the spatial mean of  $\theta$  is zero), and for  $\epsilon > 0$  the variance decays (Fig. 1). We consider the case  $\epsilon \ll 1$ , of greatest practical interest. For small  $K$ , there are three phases: (i) the variance is initially constant (if the initial scale of variation of the scalar concentration is well above the diffusive scale, as assumed here); (ii) it then undergoes a rapid superexponential decay; and (iii) it ultimately decays exponentially at a fixed rate, independent of  $\epsilon$ , as  $\epsilon \rightarrow 0$ . In the first phase, the map has not yet created gradients large enough for the small diffusion to act. In the second phase, there is a rapid exponential cascade to small scales and an associated exponential diffusion, leading to a superexponential decay. As the variance is depleted by diffusion, eventually the system settles into an eigenfunction that sets the exponential decay rate in the final phase.

The existence of these three phases is well-known,<sup>1-3,19,20</sup> but the exponential phase is the poorly understood, at least for the case of smooth flows and maps. We discuss the superexponential phase briefly in Section III, and in Section IV we describe the exponential phase. We will see that if the eigenfunction of the exponential phase decays slowly enough, then there is no superexponential phase at all.

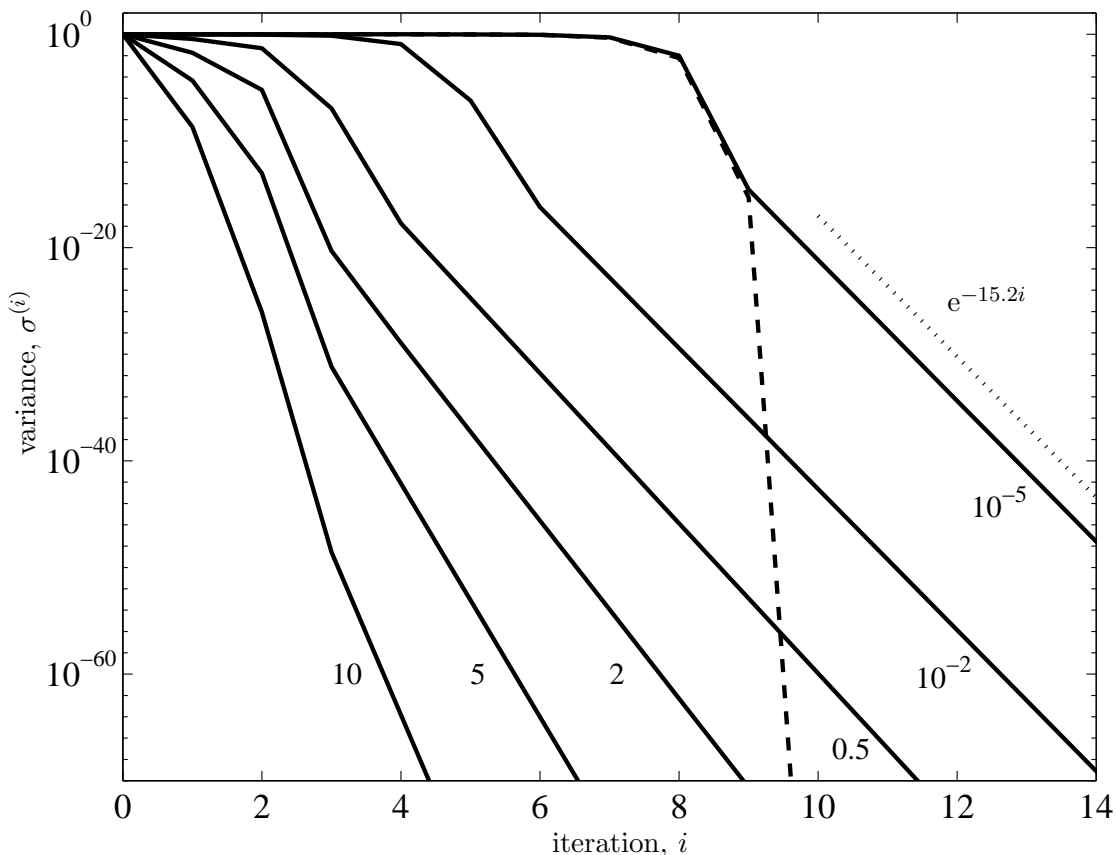


FIG. 1: Decay of total variance for varying diffusivity  $\epsilon$  and  $K = 10^{-3}$ . The onset time of decay is logarithmic in the diffusivity, but the asymptotic exponential decay rate becomes independent of the diffusivity as  $\epsilon \rightarrow 0$ . The dashed curve shows the exact superexponential solution ( $K = 0$ ) for  $\epsilon = 10^{-5}$ , and the dotted line is the single-mode value from Eq. (14).

### III. THE SUPEREXPONENTIAL PHASE

Initially, the variance is essentially constant because the tiny diffusivity can be neglected. However, there is a cascade of the variance to larger wavenumbers under the action of  $\mathcal{M}^{-1}$  in (3). (In this phase, for small  $K$ , we can neglect the  $\phi$  term in (1), so that the map  $\mathcal{M}$  is Arnold's cat map  $\mathbb{M} \cdot \mathbf{x}$ .) This is the well-known “filamentation” effect in chaotic flows: the stretching and folding action of the flow causes rapid variation of the concentration across the folds. Thus, after a number of iterations  $i_1 \simeq 1 + (\log \epsilon^{-1} / \log \Lambda^2)$ ,<sup>23</sup> where  $\Lambda = (3 + \sqrt{5})/2 \simeq 2.618$  is the largest eigenvalue of  $\mathbb{M}^{-1}$ , the diffusion can no longer be neglected. For  $\epsilon = 10^{-5}$ , we have  $i_1 \simeq 6$  (this is always an overestimate). We now describe what happens to the variance after diffusion sets in.

For small  $K$  and  $\mathbf{k}$ , we have  $J_0((k_1 + k_2)K) \gg J_1((k_1 + k_2)K)$ , so we retain only the  $Q_1 = 0$  term in the transfer matrix (9),

$$\mathbb{T}_{\mathbf{k}\mathbf{q}} = e^{-\epsilon q^2} \delta_{0,\mathbf{Q}} + \mathcal{O}((k_1 + k_2)^2 K^2); \quad (11)$$

Hence, the nonvanishing matrix elements of  $\mathbb{T}$  have  $\mathbf{k} = \mathbf{q} \cdot \mathbb{M}^{-1}$ . If initially the variance is concentrated in a single wavenumber  $\mathbf{q}_0$  (*i.e.*,  $\sigma_{\mathbf{k}}^{(0)} = 0$  unless  $\mathbf{k} = \mathbf{q}_0$ ), then after one

iteration it will all be in  $\mathbf{q}_0 \cdot \mathbb{M}^{-1}$ , after two in  $\mathbf{q}_0 \cdot \mathbb{M}^{-2}$ , etc. This amounts to the length of  $\mathbf{q}$  being multiplied by a factor  $\Lambda > 1$  at each iteration. But at each iteration the variance is multiplied by the diffusive decay factor  $\exp(-2\epsilon \mathbf{q}^2)$ , with  $\mathbf{q}$  getting exponentially larger. The total variance is given by

$$\sigma^{(i)} = \sigma^{(0)} \exp(-2\epsilon \|\mathbf{q}_0 \cdot \mathbb{M}^{-(i-1)}\|^2) \simeq \sigma^{(0)} \exp(-2\epsilon \|\mathbf{q}_0\|^2 \Lambda^{2(i-1)}), \quad (12)$$

so that the net decay is superexponential. The superexponential solution is represented by a dashed line in Fig. 1, with the solid line showing the numerical solution for the map  $\mathcal{M}(\mathbf{x})$ . The superexponential solution is valid until about the ninth iteration.<sup>24</sup> We will revisit this breakdown of the solution in Section IV.

It is to be noted that a more complicated initial condition also leads to superexponential decay, albeit with a less well-defined behavior because of the presence of several modes. Even an isotropic initial condition can be expected to have a superexponential phase: the averaging as performed in Antonsen, Jr. et al.<sup>3</sup> is problematic for a cat map in a periodic domain, because the slope of the stable (contracting) direction is irrational, and yet the wavevectors are confined to rational slopes. Hence, for finite  $\mathbf{k}$  we cannot expect the averaging to hold. However, these difficulties are of a mathematical nature specific to the present problem and do not shed much light on a more general physical situation.

#### IV. THE EXPONENTIAL PHASE

In the superexponential phase we completely neglected the effect of the wave term in the map (1). We described the action as a perfect cascade to large wavenumbers, so that the variance was irrevocably moved to small scales and dissipated extremely rapidly. There can be no eigenfunction in such a situation, since the mode structure changes completely at each iteration. This direct cascade process dominates at first, but it is so efficient that eventually we must examine the effect of the the wave term, which is felt through the higher-order Bessel functions in the transfer matrix (9).

Since the long-time exponential decay observed in the numerical results of Fig. 1 requires the existence of an eigenfunction, we may ask about the minimum requirement for this. Clearly if some scalar concentration is “left behind” in a given mode at each iteration, an eigenfunction will easily form. The question is then: Is it possible for the scalar concentration in a given wavenumber to be mapped back onto itself? This requires that the diagonal matrix element

$$\mathbb{T}_{\mathbf{q}\mathbf{q}} = e^{-\epsilon q_1^2} \delta_{0,q_1} i^{q_2} J_{q_2}(q_2 K), \quad (13)$$

be nonzero. We see from (13) that modes of the form  $\mathbf{q} = (0 \ q_2)$  are mapped to themselves with a nonvanishing amplitude at each iteration: these are the modes that depend only on the  $x_2$  coordinate. This amplitude vanishes for  $K = 0$ , since  $q_2 \neq 0$  (the  $\mathbf{q} = 0$  mode is preserved, and of no interest).

For small  $K$ , the dominant Bessel function after  $J_0$  is  $J_1$ , so the decay factor  $\mu^2$  for the variance is given by taking the magnitude of (13),

$$\mu = |\mathbb{T}_{(0 \ 1),(0 \ 1)}| = e^{-\epsilon} J_1(K) = \frac{1}{2}K + \mathcal{O}(\epsilon K, K^2). \quad (14)$$

Hence, for small  $K$  the decay rate is limited by the (0 1) mode. For  $\epsilon \rightarrow 0$ , the decay rate is independent of  $\epsilon$ . Figure 2 shows that the single-mode decay rate agrees very well

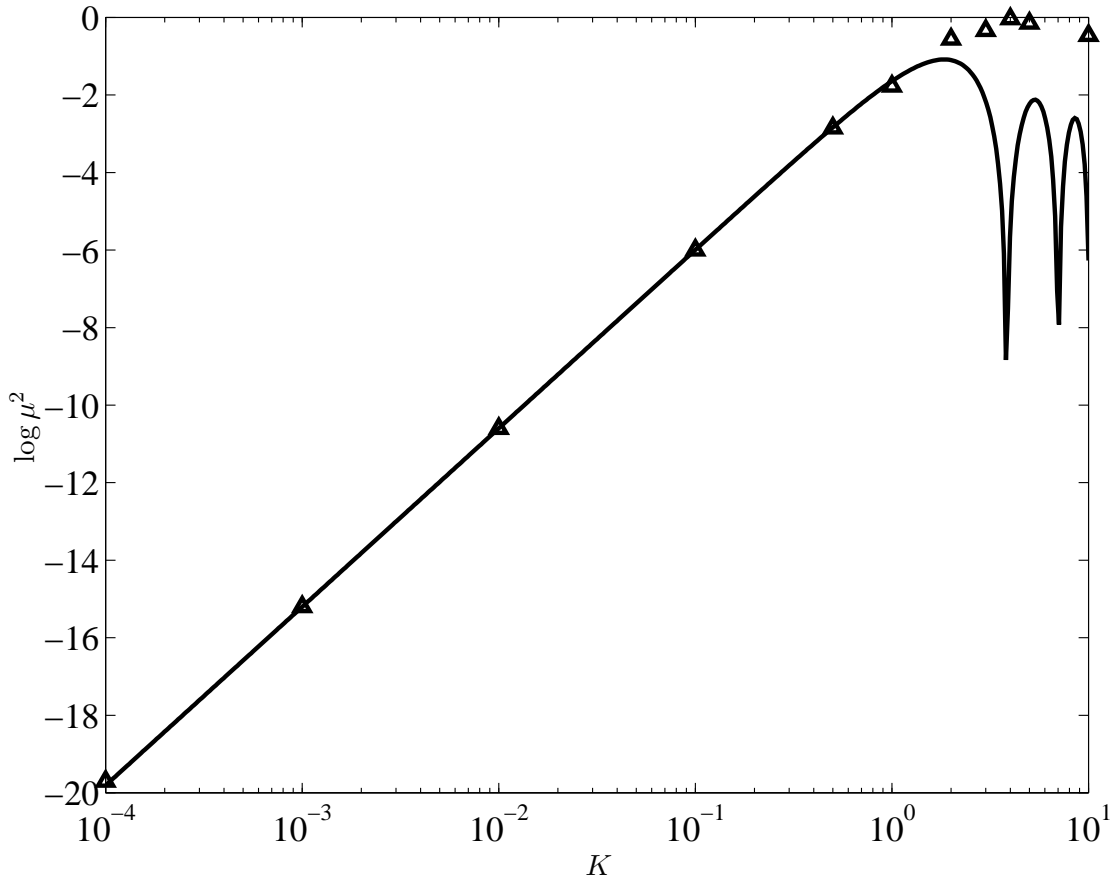


FIG. 2: Exponential decay rate  $\log \mu^2$  of the variance for  $\epsilon \rightarrow 0$ , as a function of  $K$  and. The triangles denote numerically calculated values, and the solid line is the small- $K$  expression (14).

with the numerical results even for  $K$  close to unity. In the inhomogeneous baker's map the nearly-superexponential limit is for  $\alpha \rightarrow 1/2$ , where  $\alpha$  is a parameter describing the inhomogeneity of the map. For that case the transfer matrix scales in a manner analogous to here as  $\alpha \rightarrow 1/2$ , but many more modes must be retained due to the presence of discontinuities: all the matrix coefficients decay as  $(1/2) - \alpha$ , with none clearly dominating. The single-mode approximation is thus far less accurate.

We can rule out the possibility that the decay is dominated by cycles that repeat after several iterations (that is, nonvanishing  $(\mathbb{T}^N)_{\mathbf{q}\mathbf{q}}$  for  $N > 1$ ): such cycles must depend on higher-order Bessel functions that are small compared to  $J_1(K)$ . However, as  $K$  is made larger higher-order cycles become dominant and the situation is much more complicated.

Now that the mechanism of exponential decay is understood (for small  $K$ ), we can go back and describe the condition for breakdown of the superexponential solution discussed at the end of Section III. The superexponential decay depletes the variance very rapidly until all that is left is variance in the exponentially decaying mode  $\mathbf{k}_0 := (0 \ 1)$ . The superexponential phase thus ends when the variance at large wavenumbers equals that in mode  $\mathbf{k}_0$ . Assuming that the variance resides entirely in the  $\mathbf{k}_0$  mode initially, the condition for this is

$$\mu^{i_2} = \exp(-\epsilon \|\mathbf{k}_0 \cdot \mathbb{M}^{-(i_2-1)}\|^2), \quad (15)$$

where  $\mu$  is the decay factor of the variance in the  $\mathbf{k}_0$  mode, given by Eq. (14), and the right-

hand side is the superexponential solution (12). After substituting  $\|\mathbf{k}_0 \cdot \mathbb{M}^{-(i_2-1)}\| \simeq \Lambda^{i_2-1}$ , Eq. (15) must be solved numerically for  $i_2$ : for  $K = 10^{-3}$  and  $\epsilon = 10^{-5}$ , we have  $i_2 \simeq 9.2$ . This is in fine agreement with the transition from superexponential to exponential in Fig. 1.

If  $\epsilon \ll 1$ , Eq. (15) has the approximate solution

$$i_2 \simeq 1 + \frac{\log(\epsilon^{-1} \log \mu^{-1})}{\log \Lambda^2}, \quad (16)$$

which gives  $i_2 \simeq 8$  for  $K = 10^{-3}$ ,  $\epsilon = 10^{-5}$ . Subtracting  $i_1 = 1 + \log \epsilon^{-1} / \log \Lambda^2$ , the onset of the superexponential phase (Section III), we find that the duration of the superexponential phase is roughly

$$i_2 - i_1 \simeq \frac{\log \log \mu^{-1}}{\log \Lambda^2}, \quad (17)$$

which is independent of  $\epsilon$  (at leading order), and has a weak dependence on the decay rate  $\log \mu$ . Unless  $\mu$  is very small (recall that  $0 < \mu < 1$ ), the superexponential phase is very short. In fact, for  $\log \mu^{-1} < 1$  the decay of the  $(0 \ 1)$  mode is slow enough that there is no superexponential phase at all, as indicated by the negative right-hand side in (17). We can thus speculate that it is unlikely that the superexponential phase can be observed in experiments, since there  $\mu$  tends to be close to unity.

Note that  $\epsilon$  has to be extremely small for (17) to hold: for  $K = 10^{-3}$ ,  $\epsilon = 10^{-5}$ , (17) gives  $i_2 - i_1 \simeq 1$ , whereas the unapproximated (numerical) result is  $i_2 - i_1 \simeq 2.2$ . The error on (16) and (17) scales as  $\log \log \epsilon^{-1}$ .

## V. VARIANCE SPECTRUM OF THE EIGENFUNCTION

The long-wavelength mode discussed in Section IV is the bottleneck that determines the decay rate (for small  $K$ ). But this mode does not dominate the structure of the eigenfunction. In fact, a very small amount of the total variance actually resides in that bottleneck mode: the variance is concentrated at small scales. We now derive the variance spectrum of the eigenfunction.

The variance is taken out of the  $(0 \ 1)$  mode in the same manner as described in Section III: there is a cascade from that mode to larger wavenumbers through the action of  $\mathbb{M}^{-1}$ . Neglecting the  $K$  term, the cascade proceeds from  $\mathbf{k}_0 = (0 \ 1)$  to  $\mathbf{k}_1, \mathbf{k}_2, \mathbf{k}_3, \dots$  etc., as

$$(0 \ 1) \rightarrow (-1 \ 2) \rightarrow (-3 \ 5) \rightarrow (-8 \ 13) \rightarrow \dots \quad (18)$$

The  $\mathbf{k}_n$  become more and more aligned with the stable (contracting) direction of the map as we proceed down the cascade. The amplitude of the wavenumber is multiplied at each step by a factor  $\Lambda = (3 + \sqrt{5})/2 \simeq 2.618$ , the largest eigenvalue of  $\mathbb{M}^{-1}$ .

The exponential decay rate suggests that the scalar concentration is in an eigenfunction of the advection–diffusion operator. Assuming this to be the case, Fig. 3 illustrates the transfer of variance between modes for an iteration of the map. At each iteration, the eigenfunction property implies that the variance in each wavenumber is decreased by a uniform factor  $\mu^2 < 1$ . This is illustrated by the vertical arrows in Fig. 3. The dashed arrows do not represent a direct transfer of variance, since for small  $K$  only the variance in the  $\mathbf{k}_0$  mode is actually mapped back onto itself after one iteration (this is denoted by a solid vertical arrow). Rather, there is an *effective* (indirect) transfer occurring because of

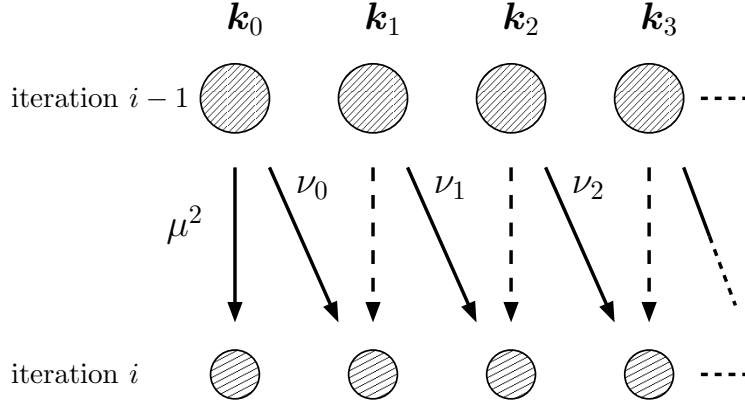


FIG. 3: Schematic representation of the cascade of variance for an eigenfunction. The solid arrows represent a direct transfer of concentration, the dashed an “effective” transfer of amplitude  $\mu^2$  due to the eigenfunction property. In our approximation, only the  $\mathbf{k}_0$  mode has a direct transfer of concentration to itself.

the cascade (18): most of the variance in each mode is mapped to the next one down the cascade following the diagonal arrows in Fig. 3.

The decrease in variance for each of the diagonal arrows is diffusive and is given by the factor  $\nu_n = \exp(-2\epsilon \mathbf{k}_n^2)$ . If we denote by  $\sigma_{\mathbf{k}_n}^{(i)} := |\hat{\theta}_{\mathbf{k}_n}^{(i)}|^2$  the variance in mode  $\mathbf{k}_n$  at the  $i$ th iteration, we have

$$\sigma_{\mathbf{k}_n}^{(i)} = \mu^2 \sigma_{\mathbf{k}_n}^{(i-1)}, \quad n = 0, 1, \dots, \quad (19a)$$

$$\sigma_{\mathbf{k}_n}^{(i)} = \nu_{n-1} \sigma_{\mathbf{k}_{n-1}}^{(i-1)}, \quad n = 1, 2, \dots \quad (19b)$$

These two recurrences can be combined to give

$$\sigma^{(i)}(\mathbf{k}_n) = \frac{\nu_{n-1} \nu_{n-2} \cdots \nu_0}{\mu^{2n}} = \mu^{-2n} \exp\left(-2\epsilon \sum_{m=0}^{n-1} \mathbf{k}_m^2\right), \quad (20)$$

where the *relative variance* in the  $n$ th mode is defined as  $\sigma^{(i)}(\mathbf{k}_n) := \sigma_{\mathbf{k}_n}^{(i)} / \sigma_{\mathbf{k}_0}^{(i)}$ . The magnitude of the wavenumber is given by the exponential recursion,

$$\|\mathbf{k}_n\| \simeq \Lambda \|\mathbf{k}_{n-1}\| \implies \|\mathbf{k}_n\| \simeq \Lambda^n \|\mathbf{k}_0\| = \Lambda^n, \quad (21)$$

which allows us to solve for  $n$ ,

$$n = \log \|\mathbf{k}_n\| / \log \Lambda \quad (22)$$

and rewrite (20) as

$$\sigma^{(i)}(\mathbf{k}_n) \simeq \|\mathbf{k}_n\|^{-2 \log \mu / \log \Lambda} \exp\left(-2\epsilon \mathbf{k}_n^2 / \Lambda^2\right), \quad (23)$$

where we retained only the  $\mathbf{k}_{n-1}^2$  term of the sum in (20) and used (21). The right-hand side of Eq. (23) for the relative variance does not (and should not if we really have an eigenfunction) depend on the iteration number,  $i$ , and depends only on  $n$  through  $\mathbf{k}_n$ . We thus let  $\mathbf{k}_n$  be a continuous variable  $\mathbf{k}$ , with  $\mathbf{k} = k(\cos \theta, \sin \theta)$ , and drop  $i$ ; from Eq. (23) we then have

$$\sigma(k, \theta) = \tilde{\sigma}(k) k^{-1} \delta(\theta - \theta_0), \quad (24)$$



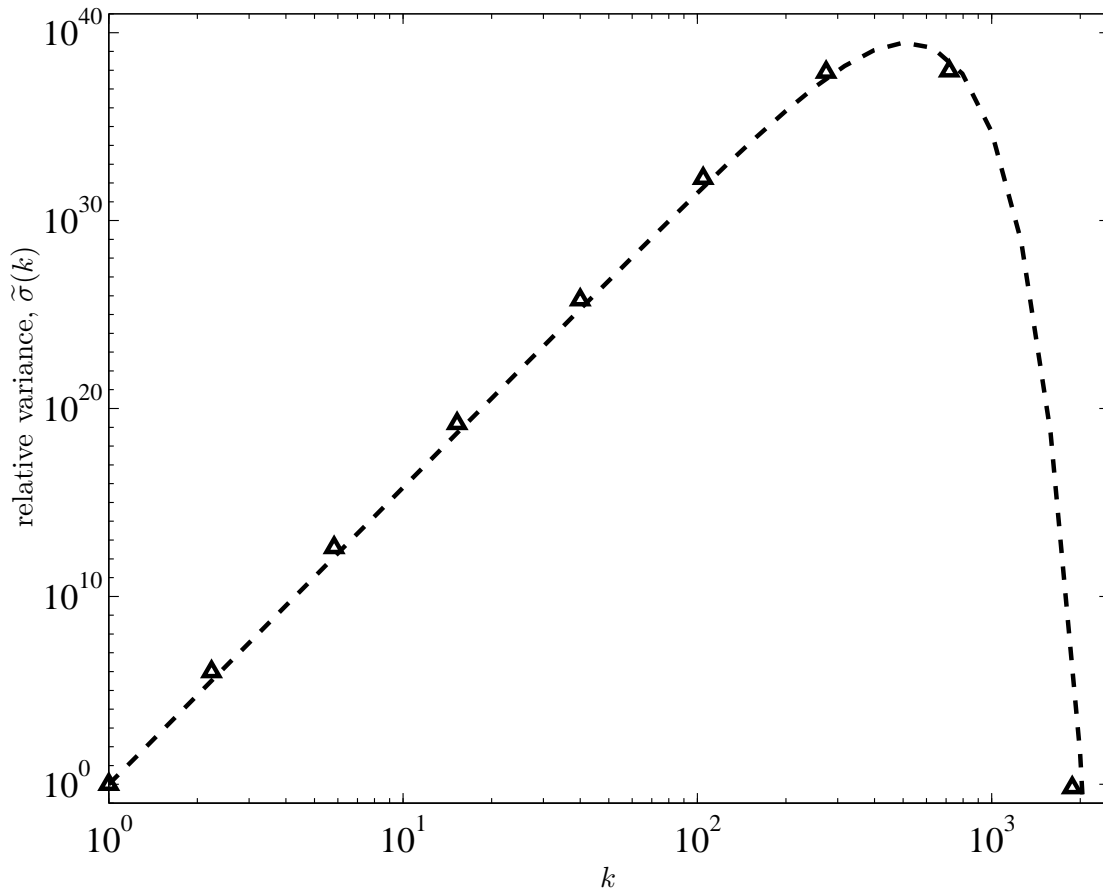


FIG. 4: Spectrum function of relative variance after 12 iterations for  $K = 10^{-3}$ ,  $\epsilon = 10^{-4}$ . The dashed line is the theoretical curve given by (25), and the triangles are numerical results.

the spectrum of relative variance, with

$$\tilde{\sigma}(k) = k^{2\zeta} \exp(-2\epsilon k^2/\Lambda^2), \quad \zeta := -\log \mu / \log \Lambda. \quad (25)$$

The factor  $k^{-1} \delta(\theta - \theta_0)$  in (24) reflects the alignment of the vectors  $\mathbf{k}$  with the stable (contracting) direction of  $\mathbb{M}$ , which is at an angle  $\theta_0$ . We thus have essentially a one-dimensional spectrum. The spectrum function then satisfies

$$\tilde{\sigma}(k) = \int \sigma(k, \theta) k d\theta. \quad (26)$$

The spectrum function (25) is plotted in Fig. 4 and compared with numerical results for small  $K$ , showing excellent agreement. Since  $\mu^2 < 1$  and  $\Lambda > 1$ , we conclude that  $\zeta > 0$  always. This implies that there is more variance at the large wavenumbers than at the slowest-decaying mode  $\mathbf{k}_0$ . The slope of the spectrum  $\tilde{\sigma}(k)$  is considerably shallower than the Batchelor  $k^{-1}$  spectrum,<sup>21</sup> consistent with the results for the baker's map.<sup>1</sup> This reflects the extreme efficiency of the cascade, a consequence of the nearly-uniform stretching, in that small scales are generated with great ease and the spectrum is therefore skewed towards large wavenumbers.

To know just how much more variance is at the large wavenumbers, we find the maximum of (25), which is at

$$k_m = \Lambda (\zeta/2\epsilon)^{1/2}, \quad \sigma(k_m) = k_m^{2\zeta} e^{-\zeta} = k_m^{2\zeta} \mu^{\log \Lambda}. \quad (27)$$

The peak wavenumber thus scales as  $\epsilon^{-1/2}$ , the same scaling as the dissipation scale. From (27), the relative variance in that peak wavenumber scales as  $\epsilon^{-\zeta}$ . The wavenumber  $k_m$  gives an indication of the largest wavenumber that must be included in a numerical calculation to capture the decay of variance correctly. However, if the truncation size is smaller, the decay rate in the exponential phase is still captured properly, since it is determined by the (0 1) mode.

## VI. DISCUSSION

We summarize the three phases of chaotic mixing in smooth flows for the case of small diffusivity. In the first phase the variance is approximately conserved, and the chaotic flow (or map) creates large gradients in the scalar concentration through its stretching and folding action. This is usually called the *stirring* phase. In the second phase, the variance (that is, the squared-amplitude of each mode with the total mean subtracted) starts to decrease superexponentially, because the exponential cascade to small scales is compounded by the exponential efficiency of diffusion (Section III). This is the first of two *mixing* phases (superexponential and exponential), where diffusion plays an important role. This superexponential phase might not occur if the exponential decay rate of the slowest-decaying eigenfunction is slow enough. For very small diffusivity, the duration of the superexponential phase is independent of diffusivity.

Unless the stretching is completely uniform, the superexponential phase comes to an end because though it rapidly depletes any variance contained in the small scales, some is left behind because of dispersion. What remains is the eigenfunction of the advection–diffusion operator with the largest eigenvalue (all eigenvalues have modulus less than one), which then decays exponentially. The decay rate of this eigenfunction is determined by its slowest-decaying part, in the present case the (0 1) mode (Section IV). The structure (spectrum) of this eigenmode is readily described as a balance between the eigenfunction property (modes are mapped to themselves with uniform amplitude) and a cascade to large wavenumbers (Section V). In the present case of a map with nearly uniform stretching, the spectrum of the eigenfunction has most of its variance concentrated at large wavenumbers, even though the small wavenumber mode (0 1) dictates the rate of decay.

The decay rate of variance is outrageously fast in a map so close to being superexponential. Nevertheless, the manner in which the asymptotic regime is attained and the possibility of analytic results provide insight into the formation of the eigenfunction through the interplay of the slowest-decaying mode and the cascade to large wavenumbers. As  $K$  is made larger, the decay rates are more reasonable and a remnant of the mechanism presented here still applies.

The decay rate in the present case is completely unrelated to the Lyapunov exponent or its distribution. For small  $K$ , the distribution of the Lyapunov exponent is peaked at  $\log \Lambda$  and has a very narrow standard deviation. But here the asymptotic exponential decay rate is of order  $\log K$ , so the decay becomes faster as  $K \rightarrow 0$ . This is due to the system being close to the uniform stretching (cat map) limit, which is unlikely to be the case in

physical situations. Any theory based on the distribution Lyapunov exponents cannot in this case predict the decay rate, since a *global* mode dominates. For the theory of Antonsen, Jr. et al.<sup>3</sup>, there is the further problem that, as in Fereday et al.<sup>1</sup>, averaging over angles is not possible here, since for small  $K$  the stable manifold and the gradient of the initial condition have a nearly constant angle with respect to each other. If the initial condition itself is taken as isotropic, then the irrationality of the slope of the contracting direction becomes problematic (Section III).

Sukhatme and Pierrehumbert<sup>17</sup> point out that what determines the regime of decay (*i.e.*, eigenfunction or local) is the scale of the initial scalar concentration. In our case, as we make that initial scale smaller we find the same asymptotic decay rate. This is due to a weak dispersion (due to the wave) from the large to the small wavenumbers which allows the system to develop its preferred (slowest-decaying) large-scale eigenfunction. The only way to get a faster rate is to completely remove the slowest-decaying eigenfunction from the initial condition, which never happens in practice. A smaller initial scale of variation does however lead to faster overall decay because its effect is to lengthen the initial superexponential scale. This is because the weak dispersion needs time to build the eigenfunction to an amplitude where it can rise above the other ambient modes.

The large-scale eigenfunctions can lead not only to faster decay but also slower (as in Fereday et al.<sup>1</sup>), when compared to local, Lyapunov-exponent based approaches.<sup>3,4,6</sup> In both cases, it is the highly-ordered nature of the system (due to the large-scale, coherent nature of the initial scalar field and flow, but also to periodic boundary conditions and walls) that gives the discrepancy. We also observe a slower decay for larger  $K$ , but no analytical theory has yet been developed to adequately describe that regime.

We observe numerically that as  $K$  is made large the spectrum of variance tends to concentrate in small wavenumbers, possibly due to the presence of a strong dispersion competing with the direct cascade to small scales.<sup>22</sup> In that limit the cascade to large wavenumbers is no longer described by the linear part  $M$  of the map, so there is no clear separation between the eigenfunction property and the cascade. An investigation of the decay rate and spectrum in this large  $K$ , wave-dominated limit will be the subject of future work.

### Acknowledgments

The authors thank A. H. Boozer, J. P. Gollub, G. A. Voth, and D. Lazanja for helpful discussions, and two anonymous referees for very constructive comments. J.-L.T. was supported by the National Science Foundation and the Department of Energy under a Partnership in Basic Plasma Science grant, No. DE-FG02-97ER54441.

- 
1. D. R. Fereday, P. H. Haynes, A. Wonhas, and J. C. Vassilicos, Phys. Rev. E **65**, 035301(R) (2002).
  2. A. Wonhas and J. C. Vassilicos, Phys. Rev. E **66**, 051205 (2002).
  3. T. M. Antonsen, Jr., Z. Fan, E. Ott, and E. Garcia-Lopez, Phys. Fluids **8**, 3094 (1996).
  4. E. Balkovsky and A. Fouxon, Phys. Rev. E **60**, 4164 (1999).
  5. M. Chertkov, G. Falkovich, and I. Kolokolov, Phys. Rev. Lett. **80**, 2121 (1998).
  6. D. T. Son, Phys. Rev. E **59**, R3811 (1999).

7. J. D. Farmer, E. Ott, and J. A. Yorke, *Physica D* **7**, 153 (1983).
8. J. M. Finn and E. Ott, *Phys. Rev. Lett.* **60**, 760 (1988).
9. J. M. Finn and E. Ott, *Phys. Fluids B* **2**, 916 (1990).
10. B. Williams, D. Marteau, and J. P. Gollub, *Phys. Fluids* **9**, 2061 (1997).
11. G. A. Voth, G. Haller, and J. P. Gollub, *Phys. Rev. Lett.* **88**, 254501 (2002).
12. G. A. Voth and J. P. Gollub, private communication.
13. H. Aref, *J. Fluid Mech.* **143**, 1 (1984).
14. D. Rothstein, E. Henry, and J. P. Gollub, *Nature* **401**, 770 (1999).
15. R. T. Pierrehumbert, *Chaos* **10**, 61 (2000).
16. R. T. Pierrehumbert, *Chaos Solitons Fractals* **4**, 1091 (1994).
17. J. Sukhatme and R. T. Pierrehumbert, *Phys. Rev. E* **66**, 056032 (2002).
18. V. I. Arnold, *Mathematical Methods of Classical Mechanics* (Springer-Verlag, New York, 1989), 2nd ed.
19. J.-L. Thiffeault, *Phys. Lett. A* (2003), in press, arXiv:nlin.CD/0105026.
20. T. Elperin, N. Kleeorin, I. Rogachevskii, and D. Sokoloff, *Phys. Rev. E* **63**, 046305 (2001).
21. G. K. Batchelor, *J. Fluid Mech.* **5**, 113 (1959).
22. S. Childress and A. D. Gilbert, *Stretch, Twist, Fold: The Fast Dynamo* (Springer-Verlag, Berlin, 1995).
23. The extra 1 in the definition of  $i_1$  appears because we diffuse at the beginning of the step in Eq. (3).
24. If, unlike the present case, the map  $\mathcal{M}$  is not chaotic, that is, it exhibits only algebraic separation of trajectories, the superexponential stage is replaced by a faster-than-exponential stage.